DOI: 10.24850/j-tyca-2021-05-04

Articles

Regional drought frequency analysis based on L-moments for the Rio Grande River Basin, Mexico

Análisis regional de frecuencia de sequías basado en L-momentos para la cuenca del río Bravo, México

Jesús Alberto Ceballos-Tavares[1], ORCID: https://orcid.org/0000-0002-6534-5515

David Ortega-Gaucin[2], ORCID: https://orcid.org/0000-0002-5336-7442

[1]Mexican Institute of Water Technology, Jiutepec, Morelos, Mexico, jesus.ceballos@posgrado.imta.edu.mx

[1]Mexican Institute of Water Technology, Jiutepec, Morelos, Mexico, dortega@tlaloc.imta.mx

Corresponding author: David Ortega-Gaucin, dortega@tlaloc.imta.mx

Abstract

In order to determine the characteristics of meteorological drought periods that occurred in the Rio Grande River Basin in the 1984-2013 period, a regional frequency analysis based on L-moments (RFA-LM) was conducted. The analysis used precipitation records from 90 weather stations, which were subject to quality control and data homogenization process. Through an iterative process, five homogeneous regions (HR) were identified according to the annual mean precipitation criterion. The probability distribution functions that best fitted the records were Gaucho (HR1) and Generalized Logistic (HR2 to HR5). Based on these functions, quantiles (annual precipitation values associated with a certain occurrence probability value) were determined, as well as precipitation deficit maps with 5, 10, 15, 20, 50 and 100 years return periods. The results indicate that meteorological drought events occur in the river basin with an average duration between 1.7 and 2.5 years, and with an average recurrence of 3.9 to 4.5 years; the longest drought period occurred between 1993-2002, and the period with the highest rainfall deficit was 2011-2012. The most affected regions are located in the states of Chihuahua and Coahuila, where the decrease levels in precipitation can exceed 80 % of the deficit, which indicates that for a return period of 100 years, more than half of the basin would show an extraordinary drought degree, which would have serious repercussions for the different socio-economic sectors.

Keywords: Meteorological drought, precipitation, regional frequency analysis, L-moments, Rio Grande River basin.

Resumen

Se realizó el análisis regional de frecuencias basado en L-momentos (ARF-LM) para determinar las características de los periodos de sequía meteorológica ocurridos en la cuenca del río Bravo durante el lapso 1984-2013. Para ello, se usaron registros de precipitación mensual de 90 estaciones climatológicas, que fueron sometidos a un proceso de control de calidad y homogeneización de datos. Mediante un proceso iterativo, se identificaron cinco regiones homogéneas (RH) de acuerdo con el criterio de precipitación media anual. Las funciones de distribución de probabilidades que mejor se ajustaron a los registros fueron Gaucho (RH1) y Logística Generalizada (RH2 a RH5). Con base en estas funciones se determinaron los cuantiles (valores de precipitación anual asociados con un determinado valor de probabilidad de ocurrencia), y se generaron mapas de déficit de precipitación con periodos de retorno de 5, 10, 15, 20, 50 y 100 años. Los resultados indican que en la cuenca se presentan eventos de sequía meteorológica con duración promedio entre 1.7 y 2.5 años, y con una recurrencia media de 3.9 a 4.5 años; el periodo de sequía más prolongado ocurrió entre los años 1993 y 2002, y el periodo que presentó el mayor déficit de lluvia fue 2011-2012. Las regiones más afectadas se ubican en los estados de Chihuahua y Coahuila, donde los niveles de disminución de la precipitación pueden superar el 80 % de déficit, lo cual indica que para un periodo de retorno de 100 años, más de la mitad de la cuenca presentaría un grado de sequía extraordinaria, lo cual tendría graves repercusiones en los distintos sectores socioeconómicos.

Palabras clave: sequía meteorológica, precipitación, análisis regional de frecuencias, L-momentos, cuenca del río Bravo.

Received: 12/05/2020

Accepted: 22/09/2020

Introduction

According to the World Meteorological Organization (OMM, 2006), drought is defined as a recurring climatic phenomenon characterized by a sufficiently extended period with abnormally dry meteorological conditions, where the lack of precipitations causes serious hydrological imbalances.

Due to its geographic location, Mexico is a vulnerable country to drought impacts; it is located within the northern belt of deserts in the world, whose existence is mainly due to the dynamics of the general circulation of the atmosphere and the features of the Earth's geomorphology. Together they generate two large atmospheric high-pressure belts located at latitudes close to 30° north and south (Ortega-

Gaucin & Velasco, 2013; Arreguín, López, Korenfeld, & Ortega-Gaucin, 2016a). Consequently, most of its territory is arid or semi-arid (52 % recording precipitations between 300-600 mm), therefore Mexico does not receive enough rainfall basically in the northern part of the country, on the contrary, the southeast region is humid with precipitations exceeding 2 000 mm per year (Esparza, 2014; Conagua, 2016).

The Rio Grande River basin is one of the most important hydrological systems in Mexico, where drought problems are a recurring condition (Linares, 2004; Ortega-Gaucin, 2013; Martínez, 2018). Its hydrological conditions are characterized by a high degree of variation referring to the availability of water resources due to the irregular and scarce precipitations in the basin, such features are influenced by the continentality, the geographic location, the orographic complexity, and the atmospheric circulation global factors (Brito-Castillo *et al*., 2010; Conagua, 2010; Núñez-López *et al*., 2013). In addition, the year-on-year precipitations variability in the region is linked, directly or indirectly, to the variable teleconnections in the sea surface temperature from the North Pacific and Atlantic regions. That is to say, phenomena such as El Niño South Oscillation (ENSO) and the Pacific Decadal Oscillation (PDO) seriously influence on seasonal rains (Rodríguez & Pineda-Martínez, 2017).

In the last decades, the social pressure on water resources in the basin has increased due to the growing urbanization and industrialization of the border area, leading to water difficulties among users (mainly agricultural), from the upper and lower parts of the basin as well as in both sides of the border with the United States (Conagua, 2014). As a

binational basin, the use of the Rio Grande River waters and most of its tributaries is subject to the dispositions established in the 1944 International Water Treaty celebrated between the United Mexican States and the United States of America. Therefore, due to the compromise for satisfying the population demands as well as to comply with such treaty, together with the increasing information about the consequences of climate change on rainfall patterns and amounts, and its runoff in the region (Arreguín, López, Velázquez, & López, 2013; Martínez, 2018), the different socio-economic sectors are highly vulnerable to drought impacts and water misuse.

The specialized literature identifies different drought types based on their origin and the impact they generate. Therefore, it is considered that drought should be treated from different standpoints, such as meteorology, agricultural, hydrological and socioeconomic (Wilhite & Glantz, 1985; Valiente, 2001; OMM, 2006). This research focuses on the specific analysis of meteorological drought, which means the precipitation deficit regarding the normal levels within the study region. When this anomaly extends in time and combines with the anthropic pressure demand for surface and groundwaters, the different socio-economic and environmental sectors undergo serious impacts.

Due to the negative consequences of this climate hazard, in recent years, there has been a change for treating it, ranging from reactive attention before the impacts caused by drought, as well as to adopting the appropriate measures in order to prevent and mitigate its effects. Particularly, this new approach was conceived within the context of risk management and disasters reduction strategies in development planning

(Bass, Ramasamy, Dey-Deprick, & Batista, 2008). In this context, the risk of a disaster due to drought events is defined as the product of hazard (represented by the drought occurrence probability) and the vulnerability level of the affected system (Wilhite, 2000; Ortega-Gaucin, De-la-Cruz, & Castellano, 2018).

Regardless of any approach used to determine the risk of social and environmental systems before a drought event, the common denominator in all methodologies is based on the need to estimate the occurrence probability of a drought event with a certain magnitude (Carrao, Naumann, & Barbosa, 2016). Generally, the most common characteristics of drought, such as intensity, duration, and geographical distribution are attained with indices and indicators of different spatial and temporary resolution (OMM-GWP, 2016). Nonetheless, the drought occurrence probability can be deduced using probabilistic hydrology tools. However, the features of arid and semi-arid regions with higher spatial and temporary precipitation variability, the influence of the external factors of decadal variability, such as the effects of ENSO, and the reduced availability of records, enforce certain restrictions regarding the selection of the most appropriate method for probabilistic adjustment (Kalma & Franks, 2003).

Thus, to solve the issues related to the limited and asymmetric availability of data in space and time, or to the absence of lengthy records for making frequency estimations with a certain reliability degree, there is a need for studying, validating, and disclosing easily implemented alternative methodologies. Such methodologies will show better frequency estimations about droughts expectancy and will generate

reliable information for decision-making (UNESCO, 2010). In this respect, the regional analysis of drought frequency based on the L-moments method has been considered as one of the best alternatives for the evaluation, estimation, and mapping of drought events occurrence probability in arid and semi-arid regions with limited availability of rainfall records, such that it pays off the lack of information in time with the richness in space it provides (Hosking & Wallis, 1997).

Thus, in recent years, the L-moment-based method has been used to determine meteorological drought characteristics in different parts of the world (Abolverdi & Khalil, 2010; UNESCO, 2010; Acuña, Felipe, Ordoñez, & Arboleda, 2011; Acuña , Felipe, & Fernández, 2015; Naranjo, 2011; Eslamian, Hassanzadeh, Abedi-Koupai, & Gheysari, 2012; Paredes, La-Cruz, & Guevara, 2014; La-Cruz, 2015). Nevertheless, Mexico has only applied it in the northwestern region of the country (Hallack & Ramírez, 2010; De-la-Cruz & Ortega-Gaucin, 2019). However, this method can be employed for solving problems that require the estimation of the occurrence frequency of certain phenomena, such as maximum daily and hourly rainfall, maximum and minimum flow rates, wind speed, solar radiation, etc. In the international scene, the method has been used to analyze the maximum floods and precipitation events (Schaefer, Barker, Taylor, & Wallis, 2007; Norbiato, Borga, Sangati, & Zanon, 2007; Báez, Prieto, & Aroche, 2016), and also for maximum temperatures (Núñez-Galeano & Giraldo-Osorio, 2016), and river flows (Vich, Norte, & Lauro, 2014; Campos-Aranda, 2014; Castillo & Ortiz, 2015).

In this context, this research is aimed to introduce the fundamentals and application of the L-moments based method, in order to analyze the

behavior of meteorological droughts, to determine the characteristics of dry periods, and to create precipitation deficit maps including different return periods, for which, the Rio Grande River basin in Mexico is used as a study case. It is intended to contribute to the understanding of the drought phenomenon in this strategic region on behalf of the country's development, and to answer some questions such as the following: In how many years should it be expected that a severe drought event affects the territory of the basin? Are there more prone regions to an extreme or exceptional drought event? Which has been the driest period in the last decades? Which is the probability that a higher deficit to 80 % of annual precipitation occurs in any year in different areas of the basin?

The truth is that, while in the practice it can be extremely difficult to predict the occurrence of a drought period, knowing the frequency, duration, and intensity of the recorded historical droughts, as well as the occurrence probability, can help the authorities and operators of hydraulic and hydrological systems to anticipate before the drought consequences (Wilhite, 2000), and will serve as a basis for the proper planning and decision-making on the water resources management of the basin.

Materials and methods

Description of the Study Location

One main feature of the Rio Grande River basin is its bi-nationality, as it is located on the border between Mexico and the United States of America (Figure 1). It belongs to the Bravo-Conchos Hydrological Region No. 24 with a territorial extension of 226 275 km^2, representing 11 % of the whole national territory. Geographically, it is located between 31° 50' and 24° 55' north latitude and 107°45' and 97°15' west longitude, covering part of the state of Chihuahua, a portion of the states of Durango and Tamaulipas and much of the states of Coahuila and Nuevo León (Semarnat, 2011).

Figure 1. Rio Grande River basin location, Mexican section.

The basin is divided into four hydrological sub-regions: Six Tributaries, High, Medium and Low Bravo; which in turn, they comprise 37 sub-basins (Semarnat, 2011), according to the 1981-2010 period, it recorded mean annual precipitation (MAP) of 371.7 mm, corresponding to 50 % of the country's MAP (739.8 mm), (Conagua, 2018). However, such precipitation value is highly variable, both temporally and geographically. Specifically, it has been recognized that cold (warm) periods of ENSO produce a winter deficit (increase) of rainfall in most of Mexico's territory and the southwestern United States (Seager *et al*., 2009). The decrease in precipitation is associated with the weakening of

humidity flows during summer in PDO (Pacific Decadal Oscillation) negative phases, although mostly in winter (Magaña, Vázquez, Pérez, & Pérez, 2003). The influence of tropical cyclones, mainly from the Gulf of Mexico produces rainfall with a significant runoff (Brito-Castillo *et al*., 2010; Núñez-López *et al*., 2013). Therefore, with such limited water availability, the development of the region, which is one of the most dynamic in the country, has led to overexploitation of groundwater aquifers and conflicts between users in need of this natural resource.

Weather Stations Selection

To obtain records on historical monthly precipitations, some stations were selected from the national climate databases (CLICOM system), belonging to the National Meteorological Service (SMN). The WMO recommended the classification criteria that were used to select stations with 80 % or more of available data for the analyzed period (1984-2013). Thus, at the time of this study, from 147 functional weather stations, 90 of them were chosen because they met the recommended criteria (see Appendix 1). Figure 2 shows their spatial distribution, showing that although they are fairly distributed within the basin, they are not present in the central and end regions thereof. However, using the analysis procedures, which will be described later, it is possible to address this lack of information.

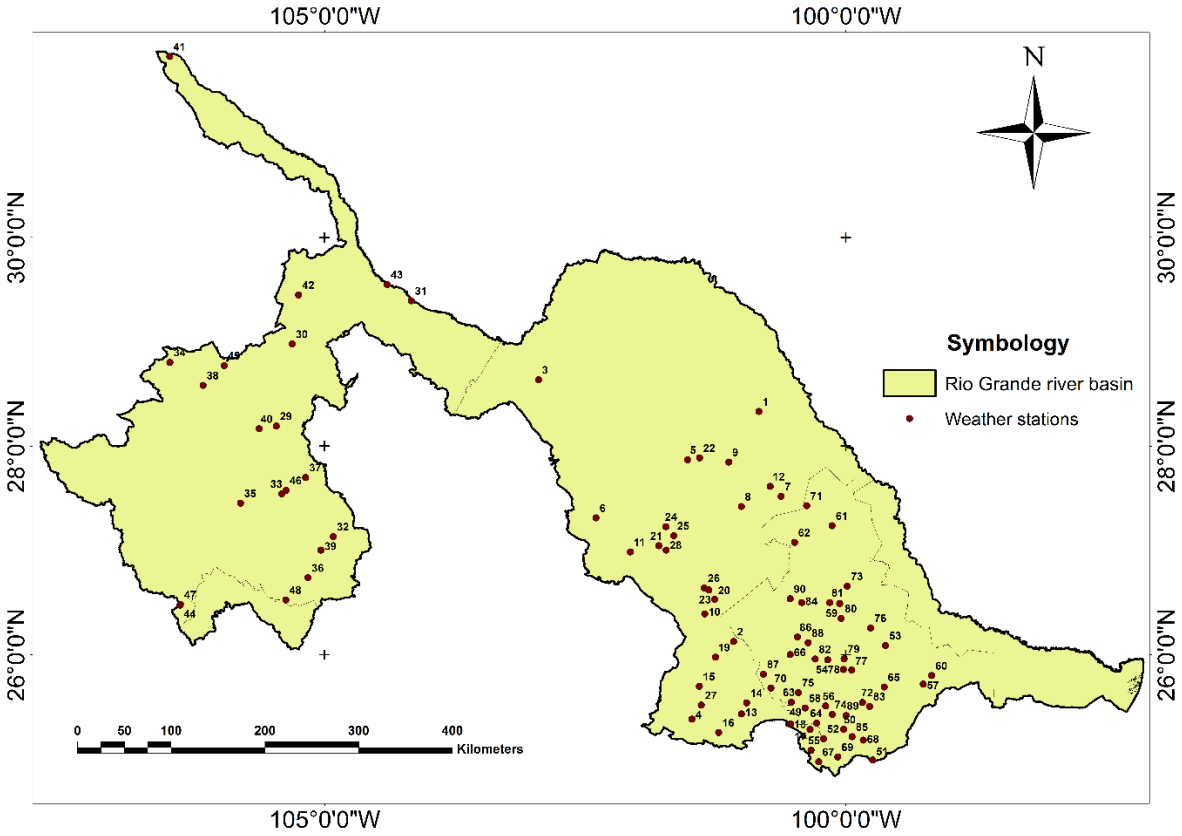

Figure 2. Location of the selected weather stations.

Fundamentals of Regional Frequency Analysis based on L-moments (RFA-LM)

L-moments (λ_i) are linear combinations of weighted probability moments (β_i), developed by Greenwood, Landwehr, Matalas and Wallis (1979), and they are statistical parameters associated with organized data. The use of L-moments involves the practice of an alternative system to traditional methods when describing the different forms of distribution functions. They are generated by linear combinations of probabilistically weighted moments. The calculation equations are the following (Stedinger, Vogel, & Foufoula-Georgiou, 1993; Hosking & Wallis, 1997):

$$\lambda_1 = \beta_o \quad (1)$$

$$\lambda_2 = 2\beta_1 - \beta_o \quad (2)$$

$$\lambda_3 = 6\beta_2 - 6\beta_1 + \beta_o \quad (3)$$

$$\lambda_4 = 20\beta_3 - 30\beta_2 + 12\beta_1 - \beta_o \quad (4)$$

The first-order linear moment (λ_1) is the variable mean; the second moment (λ_2) refers to the distribution scale which provides the data dispersion extent; the third-order linear moment (λ_3) represents the asymmetry; and finally, the fourth linear moment (λ_4) refers to kurtosis, which measures the steepness or flatness of data distribution.

Comparison of precipitation records of climate stations is carried out by the L-moments contrast in a dimensionless way, which estimates L-ratios

(τ_i). The former is obtained by dividing the linear moments with a higher scale, λ_3, and λ_4, by the distribution scale, λ_2. Therefore, it is possible to achieve a distribution form regardless of its measurement scale, allowing the evaluation of the stations with different series records. The most important values are the following:

L–CV: $\tau_2 = \lambda_2 / \lambda_1$ (5)

L–Skewness: $\tau_3 = \lambda_3 / \lambda_2$ (6)

L–Kurtosis: $\tau_4 = \lambda_4 / \lambda_2$ (7)

The RFA-LM assumes that a set of precipitation stations within a given area form a homogeneous region, if and only if, their frequency distributions are identical, varying only in the specific scale factor at each station, therefore it allows to add of all the stations belonging to a homogeneous region to improve the calculations accuracy of the quantile probability function at such stations (Hosking & Wallis, 1997; Wallis, Schaefer, Barker, & Taylor, 2007).

The RFA-LM uses three or more parameters distribution models, making it more robust than the distribution models used in typical probabilistic hydrology, which usually comprise one or two parameters.

The RFA-LM methodology, adapted by UNESCO (2010) which was employed for carrying out this research, considers the application of five

stages (Figure 3): 1) Data review and quality control, 2) Identification of homogeneous regions, 3) Selection of frequencies distribution, 4) Quantiles estimation, and 5) Mapping. The first stage was carried out aided with *Climatol* software, executed in *R* programming language; stages 2 to 4 used the *L-RAP* program (*L-Moment Regional Analysis Program*), and stage 5 used the *ArcGis*® software as described hereinafter.

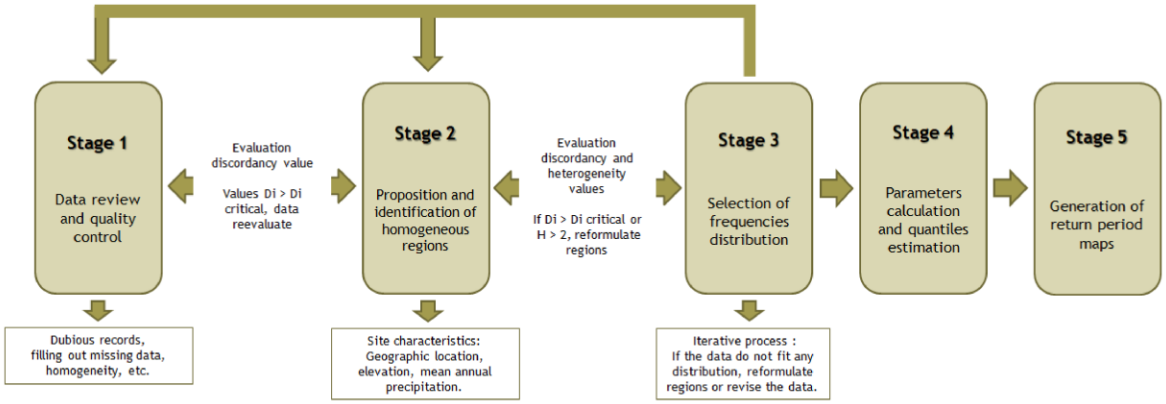

Figure 3. Flowchart of RFA-LM stages. Adapted from UNESCO (2010).

1. Data review and quality control: The purpose of this stage is to delete the dubious records associated with registration and/or transcription errors, as well as to fill out missing data. In this case, the quality control process, the homogenization, and filling out the missing data in precipitation series were carried out with *Climatol* software, version 3.1.1 (Guijarro, 2018), *R* language executed. This tool fills out the

gaps of climatic series using the Paulhus and Kohler method (Paulhus & Kohler, 1952) through a series of iterative processes that normalize the data by dividing its average values ($x=X/\mu_X$) and subtracting the averages ($x=X/\mu_X$), or with a complete standardization [$x=(X-\mu_X)/\sigma_X$], referring to μ_X and σ_X as the average and standard deviation of an X series, respectively. It also senses abnormal values, which may be due to errors while capturing information through the homogeneity test referred to as *Standard Normal Homogeneity Test* (Alexandersson, 1986). For implementing the aforementioned processes in the study basin, the basin was divided into two major zones (Figure 4) in order to achieve goodness-of-fit in the series through two independent processes, according to Guijarro's recommendations (Guijarro, 2018), concerning the proximity or closeness of the stations. Thus, 20 weather stations are located in Zone A (red color) and Zone B (blue color) comprises 70 stations. These processes resulted in new reconstructed series that were subsequently analyzed and accepted, so they were used in the RFA-LM through *L-RAP* software.

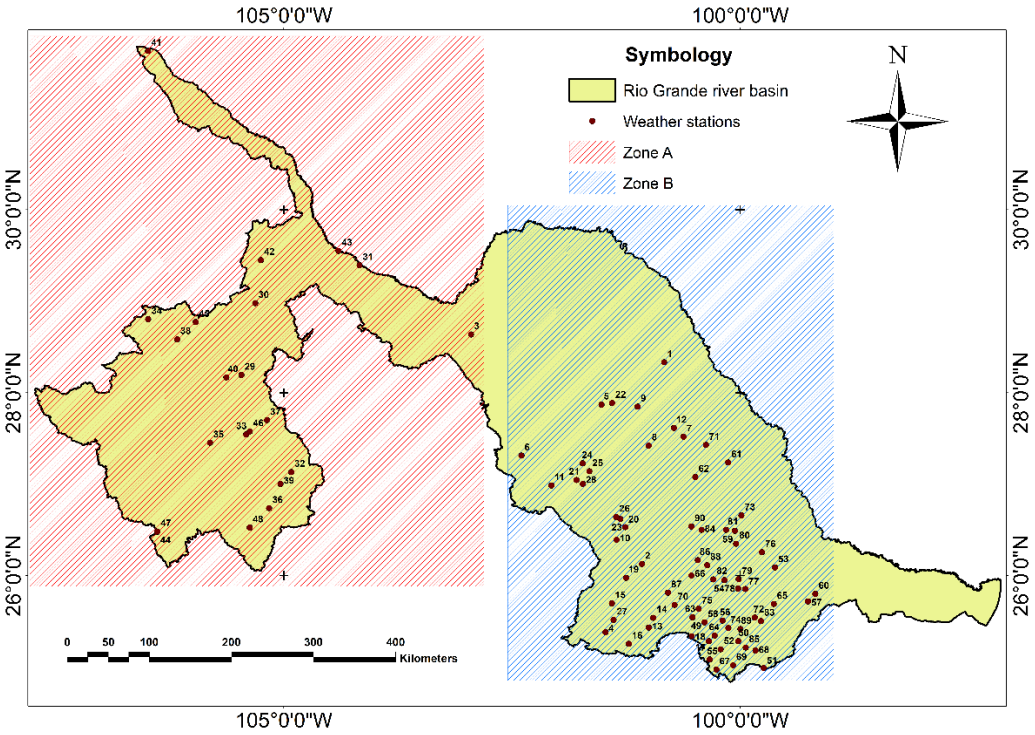

Figure 4. Basin's division for precipitation data review and quality control using Climatol.

2. Identification of homogeneous regions (HR): The aim of this stage is to form regions that satisfy the homogeneity condition. This region is defined as comprising a set of weather stations, assuming that the probabilities distribution function that governs precipitation is the same for each one of them. Regionalization is an iterative process consisting of two stages:

a) The first stage is to determine regions *a priori*, identifying stations in a geographical space with similar climate and topographical features, and using the MAP magnitude as the criterion for grouping stations. This

criterion was suggested as the best suited for grouping stations in search of a regional analysis of rainfall frequency within the context of probabilistic characterization of drought events (UNESCO, 2010). Thus, given a set of stations in one region, it is required to verify that the stations it comprises do not show discordancy properties among them. For this purpose, Hosking and Wallis (1997) introduce a discordancy measure that evaluates the extent to which the L-moments of the station are significantly adapted to the average pattern of regional L-moments:

$$D_i = \frac{1}{3} N(\mathrm{ui} - \bar{\mathrm{u}})^T A^{-1}(\mathrm{ui} - \bar{\mathrm{u}}) \qquad (8)$$

where D_i defines the discordancy average of each *i* station. Assuming that the region comprises *N* stations, where $ui = [t^{(i)} t_3^{(i)} t_4^{(i)}]^T$ are *N* column vectors, containing t, t_3, and t_4 L-moments values in each *i* station, where the superscript *T* represents the vector transposition. Then, $\bar{u}$ is the average vector of the analyzed homogeneous region and *A* represents the matrix of the sum of squares and the square products of $[(\mathrm{u_i} - \bar{\mathrm{u}})(\mathrm{u_i} - \bar{\mathrm{u}})^T]$ stations belonging to the same HR.

Reference values for D_i are established in order to evaluate whether or not a station is discordant based on a certain number of stations, and are shown in Table 1.

Table 1. Discordancy critical values according to Hosking and Wallis (1997).

Number of stations by region	Critical Value	Number of stations by region	Critical Value
5	1.333	11	2.632
6	1.648	12	2.757
7	1.917	13	2.869
8	2.140	14	2.917
9	2.329	> 15	3.000
10	2.491		

b) The second stage is to perform heterogeneity tests, which detect if the recently formed stations within a certain region, can be characterized as homogeneous. The heterogeneity measure for accepting or rejecting the proposed homogeneous regions is *H-statistic* (Hosking & Wallis, 1997), which measures the relative variability of the L-Coefficient of variation (L-CV), observed from the sample, which is determined by:

$$H = \frac{(V - \mu_v)}{\sigma_v} \tag{9}$$

where V is the standard *local L-CV* deviation, μ_V represents V the mean, and σ_V is V standard deviation.

According to Wallis *et al.* (2007), a region can be considered homogeneous when the statistical values of the test are lower than 2.0 (Table 2).

Table 2. Heterogeneity critical values according to Wallis *et al.* (2007).

Heterogeneity (H)	H Values
Homogeneous	H < 2
Possibly heterogeneous	2 < H < 3
Heterogeneous	H > 3

If the heterogeneity test fails, the discordancy measurements of each station are reviewed and a new region is formed by regrouping the discordant stations. The iterative process ends when the region is classified as homogeneous.

3. Selection of frequencies distribution: Once a region has approved the homogeneity condition, it is possible to determine the probability distribution that best fits, based on using the diagram of regional L-moments, as well as using the Z^{DIST} goodness-of-fit test (equation 10), and estimating the location, scale and shape parameters of such distribution.

$$Z^{DIST} = \frac{\left(t_4^{DIST} - t_4^R - B_4\right)}{\sigma_4} \quad (10)$$

where t_4^R represents the L-Kurtosis regional average value; B_4 is the t_4^R skewness; σ_4 is the t_4^R standard deviation; and t_4^{DIST} is the L-Kurtosis coefficient of the adjusted distribution, in which ^{DIST} refers to the probabilities distribution functions (PDF) suggested by Hosking and Wallis (1997) which include: Generalized Logistic (GL) distribution, Generalized Extreme Value (GEV) distribution, Generalized Normal (GN) distribution, Four-Parameter Kappa (Gaucho) distribution, Log-Pearson Type III (LP3) distribution and Generalized Pareto (GP) distribution.

The criterion for considering an adequate distribution is whether the absolute value of Z^{DIST} is lower than or equal to 1.64, that is to say, $Z^{DIST} \leq |1.64|$ (Hosking & Wallis, 1997).

4. Quantiles estimation: The objective of this stage is to determine quantiles, that is to say, the values of annual precipitation associated with a certain value of occurrence probability. Once the regions and frequency distributions are selected as the best suited for each case, it is proceeded to determine the necessary parameters for quantiles estimation or the quantiles complete function for a specific site. This is:

$$Q_i(F) = \mu_i \, q\,(F) \qquad i = 1, 2 \ldots n \tag{11}$$

That is to say, the quantile function $Q_i(F)$ of the place of interest, is determined from $q(F)$, which is the function of dimensionless regional quantiles (regional growth curve) calculated by the frequencies regional

analysis and multiplied by a scale factor (μ_i), which can be the average of the analyzed variable of the place of interest (UNESCO, 2010), where *i* represents each of the stations and *n* is the total number of stations in the region. This regional growth curve shows the relationship between the average local precipitation/average regional precipitation and the non-exceeding annual probability. Therefrom, it is possible to estimate the non-exceeding probability or return period (*Tr*) of any event of interest at an annual scale (La-Cruz, 2015).

5. Mapping: One of the benefits of the RFA-LM method is to easily implement the spatial mapping of quantiles, probabilities, or return periods, considering the measured and unmeasured sites. The resulting maps are highly valuable for decision-making (Wallis *et al.*, 2007; Schaefer *et al*., 2007). In this case, meteorological drought maps associated with different return periods (5, 10, 15, 20, 50, and 100 years) were generated using the geographic information system *ArcGIS*®. The interpolation method used in all maps was that of "kriging", which is based on geostatistical theory fundamentals or georeferenced variables and not assuming the normality of the analyzed variable (Oliver & Webster, 1990). This represents an advantage for handling all types of variables that are not normally distributed, either in space or in time, as is the case with precipitation.

Results and discussion

Data review and quality control

According to the analysis conducted on monthly precipitation data using *Climatol* software, data availability in the 1984-2013 period recorded 92 % average for stations in Zone A, and 88 % average for stations in Zone B, as shown in Figure 5, where it can be seen that Zone B stations have more gaps (white spaces) within the logging period.

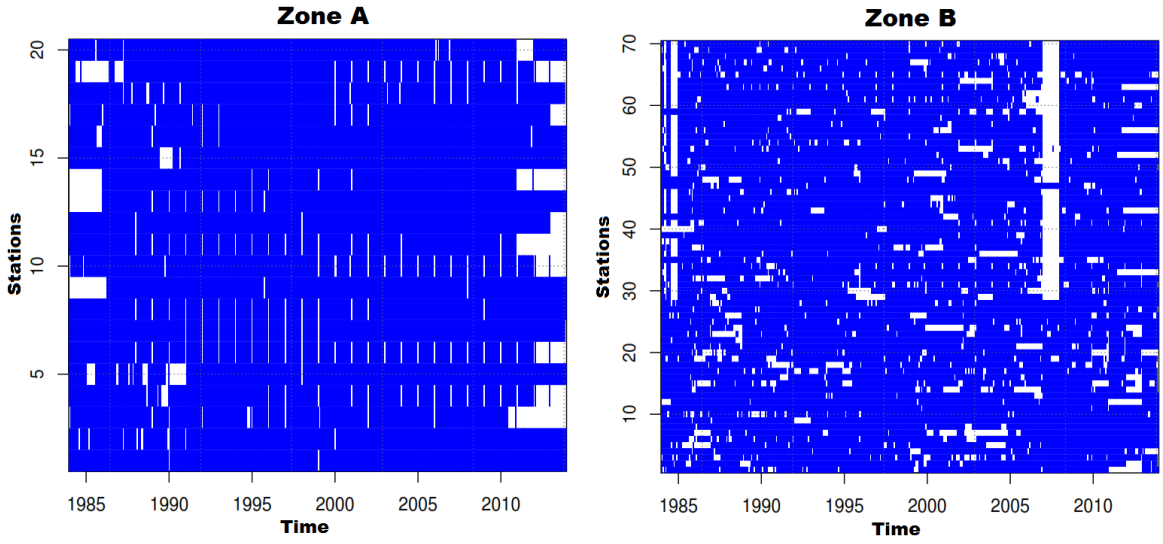

Figure 5. Availability of monthly precipitation data in weather stations (1984-2013).

After carrying out the homogenization process and filling out the missing data using the aforementioned tool, it was possible to obtain reconstructed series based on the original data of each station. As an example, Figure 6 is a graph of the "La Rosa" weather station, indicating the annual moving averages of the reconstructed series (top part), showing the original data marked in black and the filled out data in different colors (red, green, sky blue and navy blue), for each resulting series from the iterative process. The bottom part shows the applied corrections to the series in the same colors. This way in all cases, the selected and employed series were those that best represent the original values introduced into *Climatol* software, which in this exemplary case, they belong to the red series, whose correction factor is the lowermost.

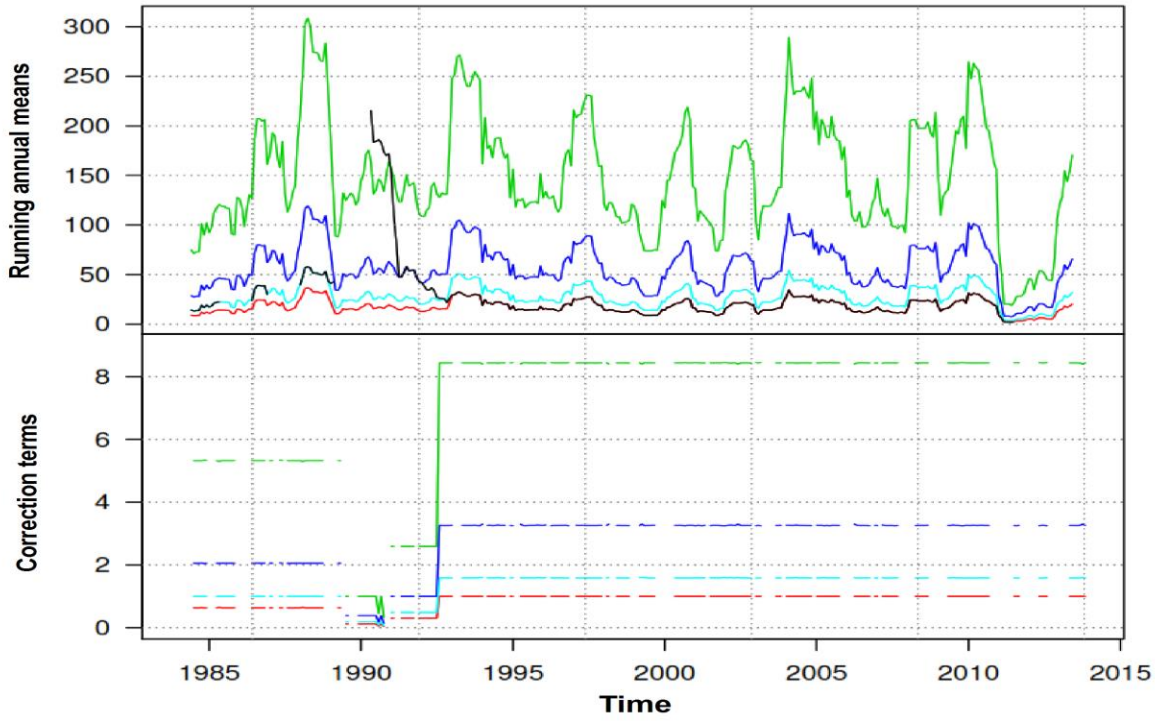

Figure 6. Reconstruction of precipitation data complete series for a weather station using Climatol.

Precipitation spatial-temporary distribution

As a result of the information process from the previous stage, Figure 7 shows the maps that illustrate the Rio Grande River basin MAP distribution during the study period. The maps were generated based on the original and reconstructed precipitation series, which show that isohyets have

changed (though minor changes) from one map to another. Both maps indicate the rainfall variation in different regions of the basin, where the lowest values are found towards the northwest region (150-250 mm), in the adjoining regions of Chihuahua with the United States, and in the central portion (251-450 mm) covering most of the state of Coahuila. The highest values are be found in the south and southeast, in the upper part of the Conchos River sub-basin (451-650 mm) and towards the states of Nuevo León and Tamaulipas (651-1 050 mm). This precipitation spatial distribution pattern is consistent with that established by Brito-Castillo *et al.* (2010), who claim the existence of a rainfall distribution pattern from south to north and from east to west in that particular monsoon region. In addition, according to Núñez-López *et al.* (2013), this distribution pattern highlights the relationship between the geographical features, the continental distance to maritime areas, and the landform complexity from precipitation occurring over the Rio Grande River basin.

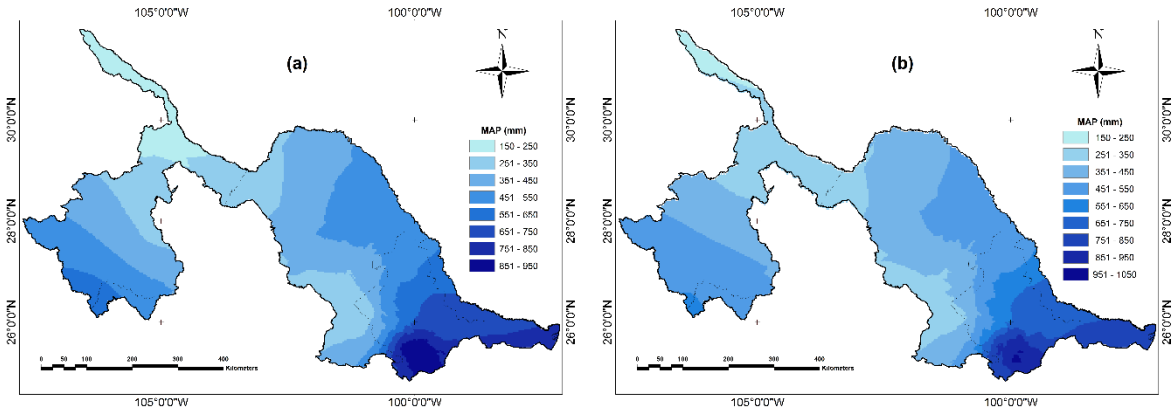

Figure 7. Mean annual precipitation (MAP) maps for the Rio Grande River basin, generated from the original (a) and the reconstructed (b) series.

Likewise, Figure 8 shows the rainfall temporary distribution throughout the year, it can be seen that the precipitation regime is characterized by the presence of a period of abundant rains, clearly defined in the summer, between June to September, thus September is the wettest month showing an average of 97.4 mm. The cumulative precipitation average during the four rainy months represents approximately 62 % of the total annual precipitation collected in the basin. These data are similar to those reported by Conagua (2018), which shows that 61.4 % of rainfall occurs among these months of the year, marking September as the rainiest of all.

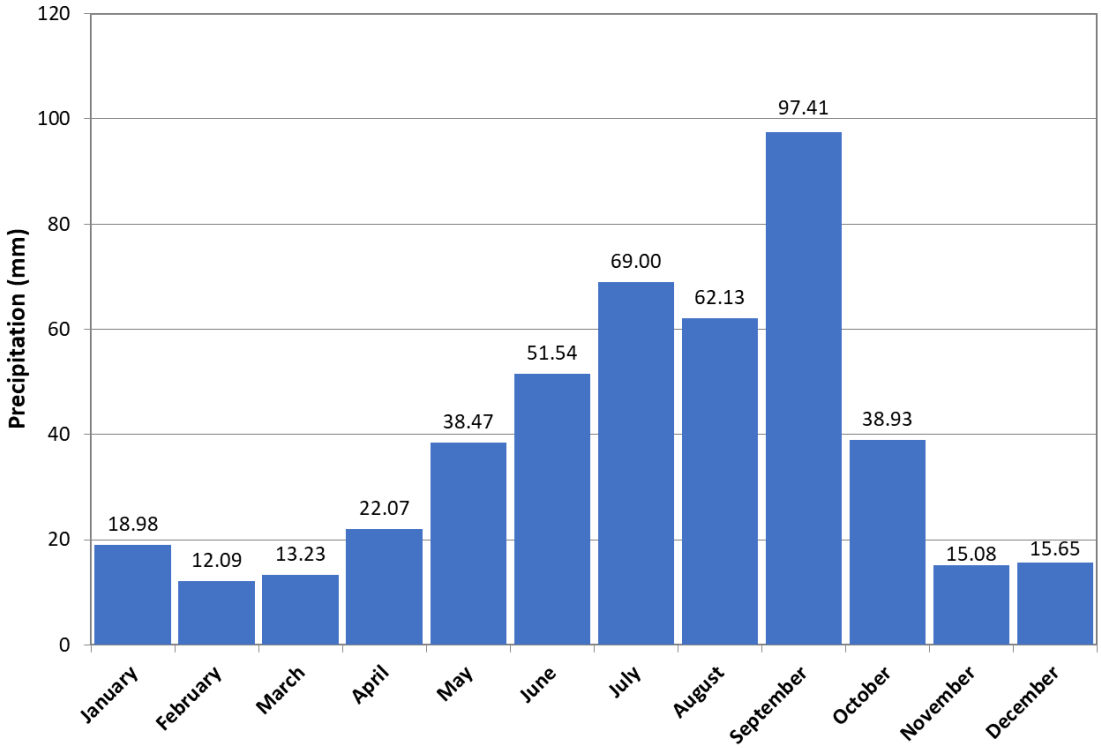

Figure 8. Distribution of monthly precipitation means in the Rio Grande River basin.

Homogeneous Regions Identification (HR)

At the beginning of the iterative process for the regionalization of the basin, it was assumed that 90 stations of the selected weather stations belonged to the same and only homogeneous region. However, the originally proposed region did not approve the homogeneity criterion according to Wallis *et al.* (2007), in that the *H* resulting value was 27.9, that is to say, far above the 2.0 critical reference value. The idea of considering all stations within a single homogeneous region was then overlooked, therefore, it was decided to group the stations into five regions based on their MAP, but while carrying out the corresponding analysis within each proposed region, several discordant stations were found. These stations were identified in each region through visual exploration using L-CV *vs* L-Skewness ratios diagrams, such as those shown in Figure 9. This graph shows a relatively uniform cloud of blue dots regarding a center value (red box), so it is possible to identify the stations whose L-moments move further from the pattern than the rest of the stations. However, graphic appreciation is a subjective method, so it was imperative to calculate D_i values for each station and the H-statistic

value for each region.

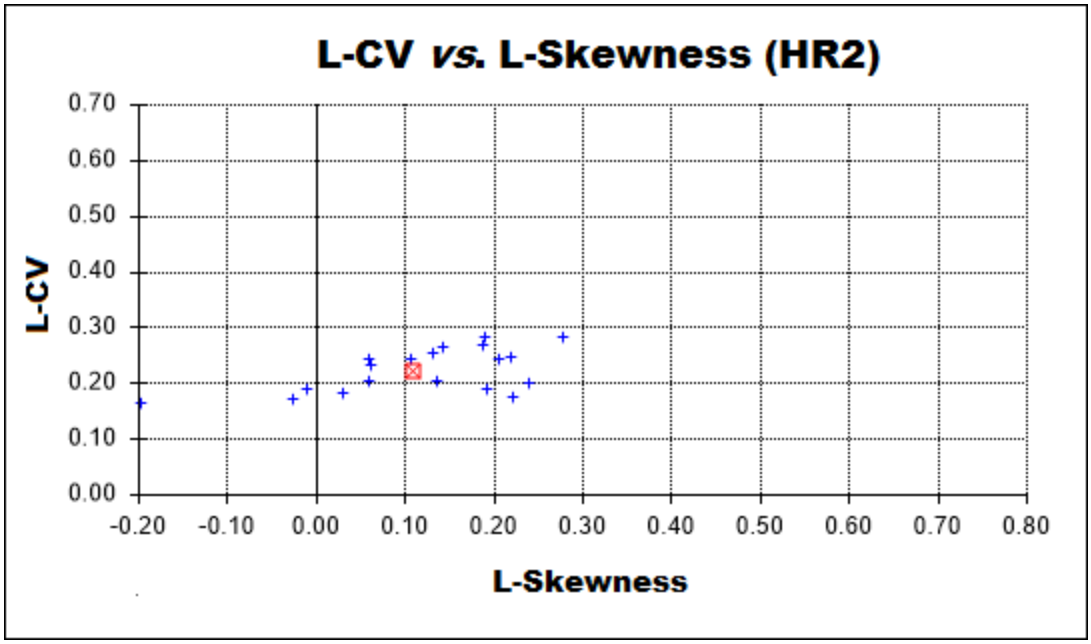

Figure 9. Example of L-CV *vs*. L-Skewness ratios diagram for a determined region.

Thus, during the iterative process, some discordant stations were relocated to a new region, as they had highly discordant values compared with the critical reference values. In this way, after several tests for different regionalization purposes, the following five regions were formed: HR1 with 24 stations and a 256.9 mm MAP; HR2 with 23 stations and a 368.8 mm MAP; HR3 with 26 stations and a 526.3 mm MAP; HR4 with 9 stations and a 675.8 mm MAP; HR5 with 8 stations and a 910.6 mm MAP (Figure 10).

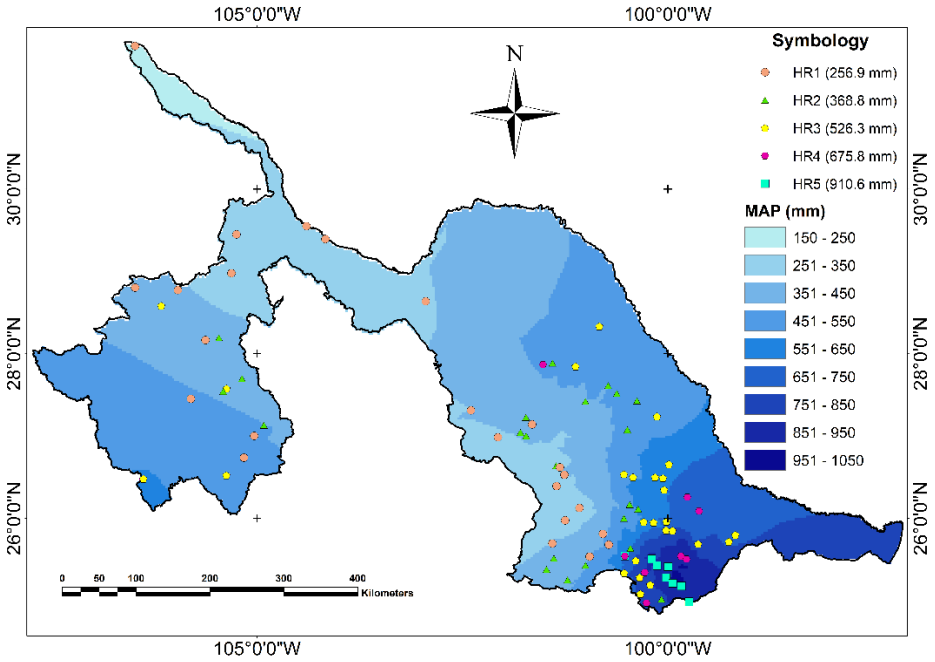

Figure 10. Spatial distribution of homogeneous regions based on the MAP criterion.

According to Hosking and Wallis (1997), homogeneous regions do not need to be geographically continuous (as can be seen in Figure 10), so stations were not forced to belong to a particular region based on their geographical location. Thus, although homogeneous stations tend to be spatially grouped, it can be seen that this condition does not apply to all of them, therefore, besides being known as "homogeneous regions", they could also be called "homogeneous groups" of stations, since some of them are located far away from the others that certainly meet the homogeneity criteria. Therefore, the natural conditions of the basin are crucial.

These regions met the homogeneity criteria according to Hosking and Wallis (1997) and Wallis *et al.* (2007), as verified on Table 3 and Table 4, which show the resulting D_i values for each station and the *H*-statistic values in each region, respectively, which in all cases, are lower than the critical reference values. Based on the foregoing, the proposed homogeneous regions were accepted, and then, it was proceeded to determine the goodness-of-fit frequencies distribution for each one of them.

Table 3. Discordancy values (D_i) for each station by homogeneous region.

HR1		**HR2**		**HR3**		**HR4**		**HR5**	
Number of Stations = 24 *Critical* D_i = 3.000		Number of Stations = 23 *Critical* D_i = 3.000		Number of Stations = 26 *Critical* D_i = 3.000		Number of Stations = 9 *Critical* D_i = 2.329		Number of Stations = 8 *Critical* D_i = 2.140	
Station	D_i	**Station**	D_i	**Station**	D_i	**Station**	**Di**	**Station**	D_i
5151	0.67	8044	0.67	5002	0.57	19002	0.64	19003	1.63
5152	0.91	5163	0.37	19024	0.09	19010	1.68	19007	0.85
19165	0.25	19170	0.70	10141	1.96	8267	2.24	19146	0.24
8247	1.61	5167	1.92	19009	0.89	19104	0.04	19015	0.60
5044	0.62	5016	2.66	19012	2.32	19033	1.04	19069	1.15
5011	1.38	8081	1.33	5149	2.63	19047	1.34	19031	1.55
5013	0.50	19096	0.96	19013	1.36	5020	1.31	19048	0.46
5158	0.45	5170	0.13	19105	1.12	19056	0.41	19173	1.51

8270	0.49	5155	1.36	19117	0.77	19140	0.29		
8049	0.77	19028	0.51	19016	1.08				
5022	0.66	19045	0.99	19018	0.14				
8254	0.64	5156	0.72	19021	0.43				
8202	2.02	5030	0.32	19022	1.02				
5140	2.06	5031	0.24	19124	0.49				
19054	0.39	19158	0.69	19042	1.06				
5164	0.59	19053	1.84	5148	0.38				
5038	2.99	5171	2.19	8185	1.59				
5142	0.87	19055	1.25	19131	1.40				
8052	0.77	5048	0.61	5033	0.12				
8099	2.26	5145	0.52	19133	0.18				
8153	1.22	5045	2.14	19134	0.74				
8156	0.89	8085	2.60	19178	0.92				
8194	1.18	8162	1.75	19063	2.39				
8213	1.48			19141	0.34				
				8322	2.74				
				8311	2.72				

Table 4. MAP and H Values by homogeneous region.

Homogeneous	**MAP**	***H***	**Classification**

Region			(Wallis *et al.*, 2007)
HR1	256.9	1.23	Homogeneous
HR2	368.8	1.39	Homogeneous
HR3	526.3	0.94	Homogeneous
HR4	675.8	1.92	Homogeneous
HR5	910.6	-0.63	Homogeneous

Selection of the goodness-of-fit probabilities distribution function (PDF)

Once the proposed HR has satisfied the homogeneity condition, it is possible to determine the regional probability distribution and its parameters, based on the use of regional L-moment-ratio diagrams, as well as using the Z^{DIST} goodness-of-fit test. To this end, the regional L-moments for each accepted HR were calculated, as shown in Table 5.

Table 5. HR regional L-moments.

Homogeneous	Regional Moments

Regions	L-CV	L-Skewness	L-Kurtosis
HR1	0.237	0.053	0.097
HR2	0.221	0.102	0.156
HR3	0.197	0.108	0.169
HR4	0.205	0.077	0.148
HR5	0.165	0.113	0.165

Likewise, the diagrams of the L-moments-ratios were attained for each region (Figure 11), relating the L-Skewness *vs* L-Kurtosis coefficients. These diagrams show the location of the regional L-moments value (red box) concerning the different PDF (color lines): GL (blue), LP3 (olive green), GEV (dark green), Gaucho (dark gray), and GP (red); where the possible distributions can be inferred and adjusted based on the data from the stations that each region comprises.

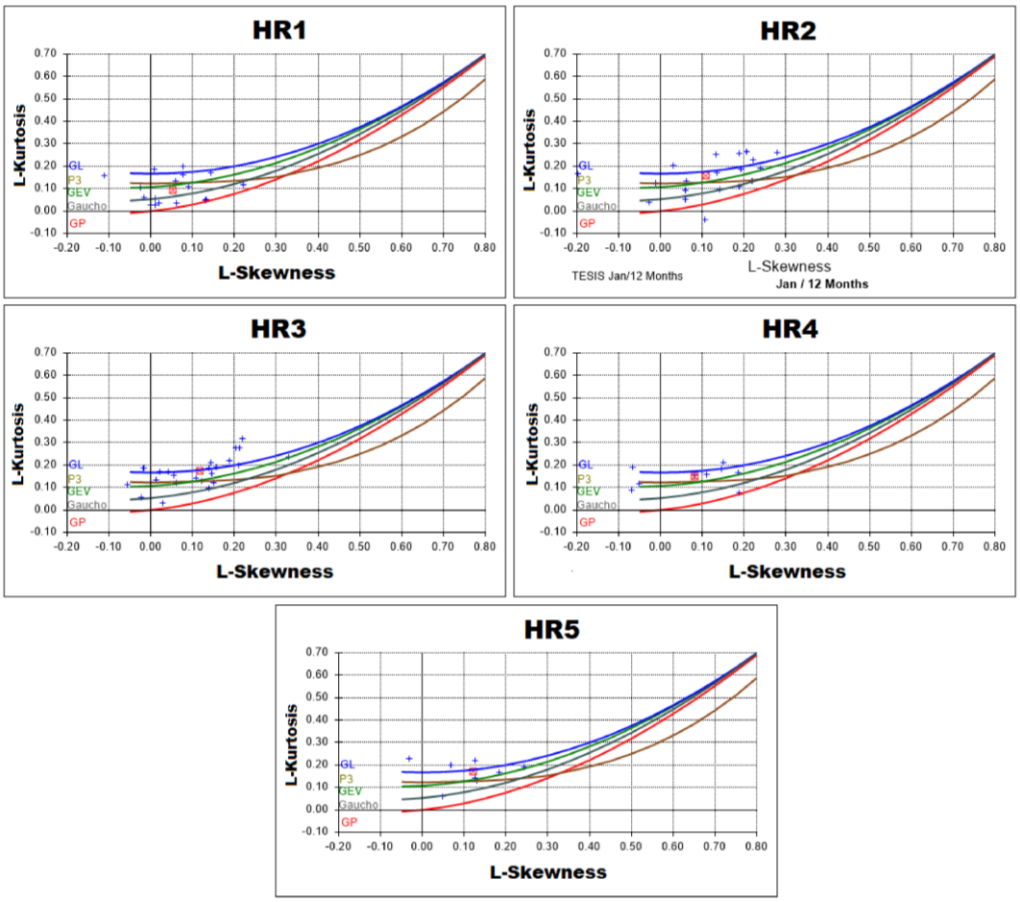

Figure 11. L-moments-ratios diagrams for each HR.

According to these diagrams, the regional L-moments behave as follows: in HR1 the mean value is between the GEV and Gaucho distributions; whereas, in HR 2, 3, 4, and 5, the mean value is located closer to the GL and GEV distributions. Thereby, it seems that any of these distributions could represent an appropriate data model. Although, as Hosking and Wallis (1997), and Peel, Wang, Vogel and McMahon (2001) point out, the final decision should not only depend on the analysis of L-

moment-ratio diagrams, so there is a need of an objective method for an accurate selection, which in this case, is the Z^{DIST} statistics.

Table 6 shows the values resulting from Z^{DIST} for each region, where those lower than the reference value are highlighted in bold ($Z^{DIST} \leq |1.64|$). Table 6 confirms the observations of previous graphs, that is to say, there is not a single PDF that fits all HRs. However, the goodness-of-fit PDF for HR1 is Gaucho distribution, whereas, for HR 2, 3, 4, and 5, the most appropriate PDF is GL, thereby, the GL distribution was selected. Appendix 2 shows the mathematical formulas describing both distributions (Gaucho and GL).

Table 6. Z^{DIST} Values for each homogeneous region.

Homogeneous Region	**Probabilities Distribution Functions**					
	Gaucho	**GEV**	**Gaucho**	**GN**	**Gaucho**	**GL**
HR1	**-1.58**	1.95	2.50	2.62	-5.13	5.68
HR2	-4.88	-1.85	-2.04	-1.66	-8.02	**1.21**
HR3	-5.74	-2.71	-3.03	-2.59	-8.88	**0.31**
HR4	-3.29	**-1.16**	**-1.05**	**-0.89**	-5.46	**1.03**
HR5	-3.08	**-1.33**	**-1.56**	**-1.28**	-4.89	**0.40**

While identifying the corresponding PDF for each region, the parameters of its location, scale, and shape were obtained, as shown in Table 7. These parameters are useful for determining quantiles for

probability values set.

Table 7. PDF Parameters for homogeneous regions.

Homogeneous Region	PFD	Parameters			
		Location	Scale	Shape (k)	Shape (h)
HR1	Gaucho	0.6745	0.6292	0.4408	0.500
HR2	GL	0.9606	0.2165	-0.1091	--
HR3	GL	0.9622	0.1922	-0.1176	--
HR4	GL	0.9722	0.2024	-0.0829	--
HR5	GL	0.9673	0.1607	-0.1217	--

Quantiles estimation

Quantiles are values associated with a given probability value, based on a cumulative probability distribution function defined by its parameters. Once the PDF was selected, the quantiles for each homogeneous region were estimated (Table 8), generating regional growth curves (Figure 12). Based on this figure it can be concluded that the return period for a year whose annual precipitation is, for example, 60 % of MAP ($P_i/PMA = 0.6$)

in the less rainy region of the basin (HR1), would be 5 years, that is to say, that period corresponds to the recurrence time of the event.

Table 8. Quantiles by homogeneous region.

HR	PDF	Quantiles																
		0.005	**0.01**	**0.02**	**0.05**	**0.1**	**0.2**	**0.3**	**0.4**	**0.5**	**0.6**	**0.7**	**0.8**	**0.9**	**0.95**	**0.96**	**0.98**	**0.99**
HR1	Gaucho	0.23	0.25	0.29	0.37	0.46	0.61	0.74	0.86	0.97	1.1	1.23	1.38	1.58	1.72	1.75	1.85	1.91
HR2	GL	0.09	0.18	0.27	0.42	0.54	0.68	0.79	0.87	0.96	1.05	1.15	1.28	1.5	1.71	1.78	2.01	2.25
HR3	GL	0.21	0.28	0.36	0.48	0.59	0.72	0.81	0.89	0.96	1.04	1.13	1.25	1.44	1.64	1.7	1.91	2.13
HR4	GL	0.1	0.2	0.3	0.44	0.57	0.71	0.81	0.89	0.97	1.06	1.15	1.27	1.46	1.65	1.71	1.9	2.1
HR5	GL	0.34	0.4	0.47	0.57	0.66	0.76	0.84	0.9	0.97	1.03	1.11	1.21	1.37	1.54	1.59	1.77	1.96

Tecnología y Ciencias del Agua

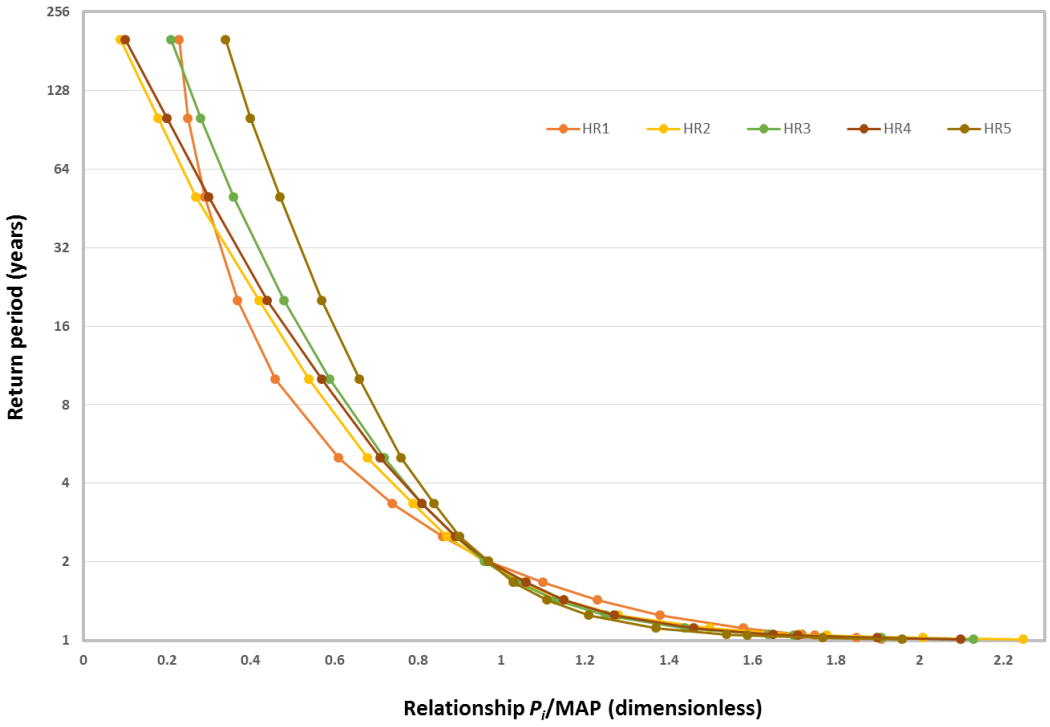

Figure 12. Regional growth curves by homogeneous region.

The 0.005, 0.01, 0.02, and 0.05 quantiles are associated with the presence of drier rainfall events with return periods of 200, 100, 50, and 20 years respectively. The use of the quantiles together with L-moments and the selected PDF parameters can be used to better determine the probability of non-excess precipitation compared to the annual mean for different return periods.

According to Table 9, for a 20-year return period (*Tr*), HR1 expects at least one event as low as 94.78 mm MAP; for the same *Tr,* HR5 expects at least one event as low as 518.70 mm MAP. Considering these 20 years,

it is observed that HR1 would have a deficit regarding its annual mean of more than 60 %; HR2, 3, and 4 would be within the range of a 50 to 60 % deficit, while HR5 would show the lowest value in the entire basin with approximately a 43 % deficit.

Table 9. L-moments and parameters for each homogeneous region and P_i for different return periods.

HR	MAP	PDF	PDF Parameter				Return Periods (Precipitation in mm)					
			Location	Scale	Shape (k)	Shape (h)	Tr 5	Tr 10	Tr 15	Tr 20	Tr 50	Tr 100
HR1	256.9	Gaucho	0.6745	0.6292	0.4408	0.500	156.6	119.0	103.6	94.7	74.5	64.8
HR2	368.8	GL	0.9606	0.2165	-0.1091	------	251.5	198.2	171.2	153.1	101.0	65.7
HR3	526.3	GL	0.9622	0.1922	-0.1176	------	377.0	310.5	276.9	254.6	190.5	147.3
HR4	675.8	GL	0.9722	0.2024	-0.0829	------	477.8	382.2	332.8	299.6	202.0	134.3
HR5	910.6	GL	0.9673	0.1607	-0.1217	------	694.1	598.7	550.5	518.7	427.2	365.7

Based on Table 9, it can be seen that the strength of drought episodes is inversely related to their frequency, that is to say, extreme events occur less frequently than moderate ones. Droughts also affect regions with lower MAP levels to a higher extent, resulting in deficit values of 31.8 % for a *Tr* 5, up to 82.2 % for a *Tr* 100 in HR2, while for HR5 in the same return periods, deficit values range from 23.8 to 59.8 %.

The aforementioned is only when considering the values reflected from each homogeneous region. However, to determine the average

duration and periodicity (recurrence) of dry periods at each region, a timely analysis was also conducted for each weather station, where the parameters of each station were determined according to the corresponding PDF, so now besides involving all stations within the same HR, the analysis was carried out with its location, scale and shape parameters, to generate precipitation deficit maps for different return periods, with the aid of its quantiles.

Dry periods analysis

To determine the type of period (dry or humid) that occurred during a particular year in each weather station, historical MAP was used as a reference, which in this case, it belongs to the normal precipitation in 30 years under study (1984-2013). Thus, based on the monthly and annual precipitation records, the characterization of meteorological drought periods was carried out for each station within the five different homogeneous regions. Then, the average duration and periodicity of dry periods were determined, and the longest period and driest year in each region were identified, as shown in Table 10.

Table 10. Recorded dry periods characteristics in each homogeneous region.

HR	Number of recorded years	Drought periods		Lengthiest drought period		Dry years	
		Average duration (years)	Average periodicity (years)	Period	Duration (years)	Driest year	% regarding the mean
HR1	30	2.5	4.4	1998-2002	5	2011	41.3
HR2	30	2.0	4.5	1993-1996	4	2011	41.6
HR3	30	2.0	4.4	1998-2001	4	2011	49.8
HR4	30	2.3	4.4	1993-1996	4	2011	51.3
HR5	30	1.7	3.9	1996-2000	5	2011	53.9

Based on this information, it is concluded that the Rio Grande River basin registers drought events with an average duration between 1.7 and 2.5 years and an average recurrence from 3.9 to 4.5 years. According to the longest drought periods duration found in each homogeneous region, it is confirmed that the longest period of meteorological drought occurred between 1993 and 2002 (with slight variations from one region to another).

These results are consistent with those presented by Velasco, Aparicio, Valdéz, Velázquez and Kim (2004), who used the Standardized Precipitation Index (SPI) and the Palmer Drought Severity Index (PDSI) to analyze meteorological drought periods in the Rio Grande tributary basins, and determined that a "persistent drought" occurred during the

1993-2001 period in the Conchos River Basin, such that the captured and stored volumes in dams reached historical minimum levels, causing serious economic impacts in the regional agricultural and livestock activities. Likewise, these results are similar to those disclosed por Núñez-López, Muñoz-Robles, Reyes-Gómez, Velasco and Gadsden-Esparza (2007), who analyzed meteorological drought events in the state of Chihuahua using the SPI index (1970-2004). It was found that the outstanding drought events occurred in the mid-to-late 1990s, considering their intensity and duration, showing negative effects on agricultural activity, as well as in the incidence of forest fires and the storage of the state's most important reservoirs. Similarly, the results also match with those submitted by Montero, Santana, Mateos and Ibáñez (2017), who analyzed extreme precipitations in the Conchos River Basin (also using the SPI index) over the 1961-2008 period and concluded that the longest and toughest drought period was in 1995-2003.

Due to the phenomenon of drought propagation, the extensive rainfall deficit can be translated into surface runoff deficit and low reservoir storage; that is to say, the meteorological drought turns into a hydrological drought (Wilhite & Glantz, 1985). Therefore, the above results are also consistent with those reported by Ortega-Gaucin (2013), who characterized the periods of historical recorded hydrological drought in the Rio Grande River basin, and concluded that in most of its territory, there was an extraordinary hydrological drought period that lasted almost fourteen years (1992-2005), and which is now recorded as the most severe and extended one. As a result of this drought, the annual volume of water used in the basin's irrigation districts (005 Delicias, 090 Bajo Río

Conchos and 103 Río Florido, Chih.; 004 Don Martín, Coahuila-Nuevo León, and 025 Bajo Río Bravo, Tamaulipas), considerably decreased: during the 1993-2005 period, an average of 1 586 hm^3 were used as irrigation waters, representing 64 % of the standard used during the 1940-1992 period (2 478 hm^3). This condition caused a significant decrease in the annual cultivated area in such irrigation districts: the 1993-2005 period registered an average of 189 710 irrigated hectares, representing 61 % of the historical irrigated areas until 1992 (308 537 hectares). The extraordinary drought also affected Mexico water deliveries from the Rio Grande River to the United States following the 1944 International Water Treaty, since in the 1993-2005 period, only 60 % of 432 hm^3 established in said Treaty as the mean annual value were supplied (*i.e.,* a total of 2 158.6 hm^3 must be delivered, in five-year cycles). Thus, since the early 1990s, Mexico began gathering a deficit in water supplies from the Rio Grande River to the United States, and according to the agreements of both governments for reducing such deficit, deliveries were partially covered in the middle of the first decade of this century and was fully settled in 2010; but repeated payment defaults on the debts for the new five-year cycle were reflected while facing the severe drought all over the northern part of the country, in 2011.

This research identified 2011 as the driest year in all regions of the basin (see Table 10), showing a precipitation deficit regarding the average that varied from one region to another from 41.3 to 53.9 %. The National Weather Service (SMN) recorded information for the same year using Mexico Drought Monitor (which is based on the analysis and interpretation

of various rates of meteorological and hydrological drought) when 80 % of the national territory underwent severe drought conditions, and the northern region was under exceptional drought conditions (Ortega-Gaucin & Velasco, 2013). Just in that year, more than 800 000 hectares of different crops were lost at the national level, representing a loss of approximately 7.75 billion pesos; and regarding livestock, mainly beef cattle, an activity intrinsically related to agriculture, about 1.3 million were lost (Cenapred, 2012), which reveals the severity of that drought.

Different drought degrees for dry periods along the Rio Grande River basin were determined based on each year's information resulting from the analyzed historical record. Therefore, a classification for drought degrees according to quintiles was proposed (Table 11).

Table 11. Meteorological drought degree classification based on quintiles.

Deficit relative to mean (%)	Drought degree
≤ 20	Light
> 20 - 40	Moderate
> 40 - 60	Severe
> 60 - 80	Extreme
> 80	Exceptional

This analysis considered the available sheet before the dry period deficit, compared with the homogeneous region mean to assign a drought degree, as shown in Table 12.

Table 12. Dry periods and drought degrees by homogeneous region.

HR	Dry periods	Accumulated deficit (mm)	Intensity (mm/year)	Available sheet before deficit (mm)	Deficit relative to mean (%)	Drought degree
HR1	1989-1989	77.4	77.4	179.6	30.1	Moderate
	1993-1996	202.1	50.5	54.8	78.6	Extreme
	1998-2002	256.6	51.3	0.4	99.8	Exceptional
	2005-2006	31.9	15.9	225.1	12.4	Light
	2009-2009	13.2	13.2	243.7	5.1	Light
	2011-2012	178.8	89.4	78.1	69.5	Extreme
HR2	1984-1984	5.2	5.2	363.7	1.4	Light
	1989-1989	88.6	88.6	280.3	24.0	Moderate
	1993-1996	231.1	57.7	137.8	62.6	Extreme
	1998-2001	211.9	52.9	157.0	57.4	Severe
	2006-2006	2.3	2.3	366.5	0.6	Light
	2009-2009	69.8	69.8	299.1	18.9	Light
	2011-2012	301.4	150.7	67.5	81.7	Exceptional
HR3	1989-1989	114.3	114.3	412.0	21.7	Moderate

	1991-1991	26.1	26.1	500.2	4.9	Light
	1994-1996	294.4	98.1	231.9	55.9	Severe
	1998-2001	286.1	71.5	240.2	54.3	Severe
	2009-2009	104.6	104.6	421.6	19.8	Light
	2011-2012	404.2	202.1	122.1	76.8	Extreme
HR4	1989-1991	264.5	88.1	411.2	39.1	Moderate
	1993-1996	385.6	96.4	290.1	57.0	Severe
	1998-2000	150.2	50.0	525.5	22.2	Moderate
	2006-2006	27.2	27.2	648.6	4.0	Light
	2009-2009	57.4	57.4	618.3	8.5	Light
	2011-2012	410.4	205.2	265.3	60.7	Extreme
HR5	1984-1985	128.4	64.2	782.2	14.1	Light
	1989-1989	105.8	105.8	804.8	11.6	Light
	1991-1991	6.3	6.3	904.3	0.6	Light
	1994-1994	87.8	87.8	822.7	9.6	Light
	1996-2000	503.2	100.6	407.4	55.2	Severe
	2006-2006	101.1	101.1	809.5	11.1	Light
	2009-2009	105.5	105.5	805.0	11.5	Light
	2011-2012	467.9	233.9	442.6	51.3	Severe

An analysis of the previous table verifies that the 2011-2012 period, which is considered in other investigations as the most severe drought event in recent years (Ortega-Gaucin & Velasco, 2013; Arreguín, López, Korenfeld, & Ortega-Gaucin, 2016b), appears nearly in all regions of the

basin in this research. It shows an intensity ranging from region to region and ranging from severe drought (with a 40-60 % deficit regarding the mean) to exceptional drought (whose deficit is higher than 80 % regarding the mean). As the cited authors mention, the most damaged states by that national drought in such period were Chihuahua and Coahuila, located in the central and western part of the Rio Grande River basin and which belong to the HR1 and HR2 regions in this study. The National Program Against Drought (Pronacose) was launched in Mexico after this dry period, which was aimed to execute a paradigmatic shift in treating drought, moving from reactions before the emergency to a preventive model focused on risks control. The fundamentals of this program —prevention and mitigation— are the basis for improving drought risk management, and to strengthen local capabilities to face the impacts with appropriate strategies (Arreguín *et al.*, 2016b).

Mapping

In order to comprehensively understand and interpret meteorological drought magnitude and its spatial-temporary distribution associated with different return periods (5, 10, 15, 20, 50, and 100 years), precipitation deficit maps were produced for each return period in the Rio Grande River basin (Figure 13).

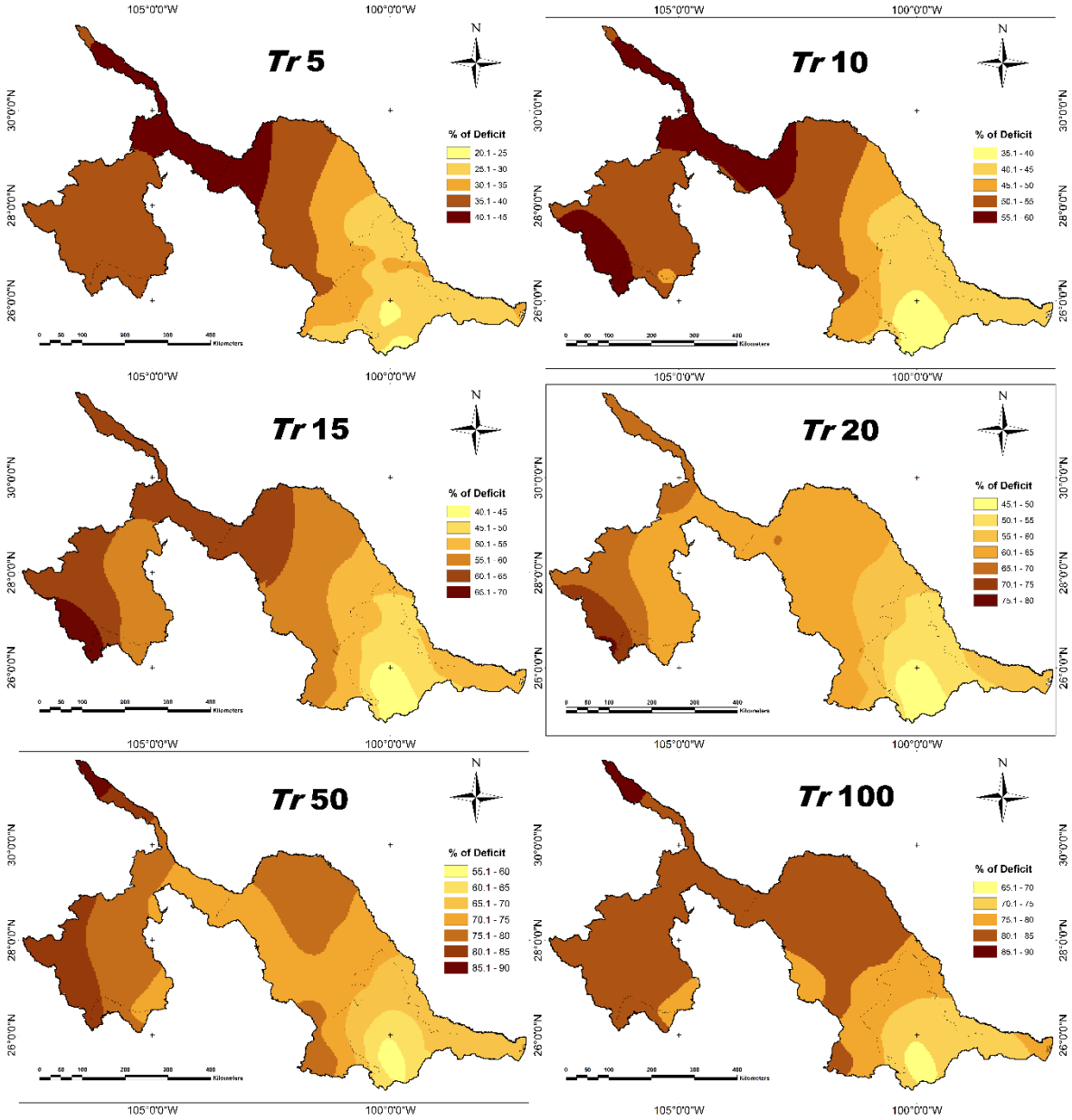

Figure 13. Precipitation deficit maps with different return periods (Tr) for the Rio Grande River basin, Mexico.

As can be appreciated from the different maps of Figure 13, the regions that would show meteorological drought with a higher rainfall deficit degree and shorter return periods would be HR1 and HR2 (which cover most of the basin in the states of Chihuahua and Coahuila). Their precipitation deficit levels vary in time up to a level of 80 % deficit, meaning that for 100 years return period, more than half of the basin will undergo an extraordinary drought degree, causing a substantial impact on different economic activities and in the population.

These results are related to those stated by Núñez-López *et al.* (2013), who point out that proximity or remoteness to coastal areas reflects a clear continentality effect, showing a decrease in precipitation values depending on how far the maritime zone lies. According to this, HR4 and HR5, located in the east part of the basin (in the states of Tamaulipas and Nuevo León) show the highest precipitation levels (601-750 mm and 751-1000 mm, respectively). As such, the generated maps from this research, reflect that HR5 is the least prone region to undergo an extreme meteorological drought degree, as precipitation tends to increase in length values near the east of the basin (Gulf of Mexico coast), besides being frequently benefited by the Atlantic tropical cyclones.

Drought degrees shown on the precipitation deficit maps are intensified as the return period increases, with extreme to exceptional droughts with up to 90 % rainfall deficit for a 100-year return period. This matches the results reported by Kim, Valdés and Aparicio (2002), who investigated drought characteristics within the Conchos River Basin through the PDSI index, finding out that the most severe drought (occurring in the 1990s), shows an associated return period of

approximately 80 to 100 years over wide areas. Likewise, it matches the results submitted by Cerano, Villanueva, Valdez, Méndez and Constante (2011), who used dendritic methods to remodel precipitation records over the past 600 years in the east region of the Rio Grande River basin (mountainous region of Coahuila and Nuevo León). One of its conclusions confirms droughts and mega-droughts occurrence with a periodicity of approximately 50 to 100 years, matching the historical records of social and economic damage caused by these droughts in Mexico, such as, the "year of hunger" drought in 1786, and the droughts before the social movements of Independence in 1810 and the Revolution in 1910, which unchained its appearance (Florescano, 2000).

Conclusions

This research describes the fundamentals and the application of the regional drought frequency analysis based on L-moments in order to determine the dry period's characteristics occurring in the Rio Grande River basin, from 1984 to 2013. Regarding the employed method, it proved to be a useful option for reporting meteorological drought analysis in arid and semi-arid regions, such as the Rio Grande River basin, characterized by its high spatial and temporary precipitation variability,

influenced by external factors on decadal variability, and with limited availability of rainfall records. Therefore, it is possible to pay off the lack of information in time with its abundance in space. Besides, the method used three or more parameters distribution models (such as the four-parameter Kappa distribution), proving to be more flexible and wide-ranging than traditional probabilistic hydrology models, which usually use one or two parameters. It is possible to make adjustments using conventional models, which could provide unacceptable results in presence of atypical values based on physical features, such as annual precipitations attributed to the ENSO phenomenon, however, L-moments are highly insensitive to those atypical values, therefore, they are statistically more robust.

On the other hand, concerning the results, the development of the proposed methodology allowed us to identify five homogeneous climate regions according to the mean annual precipitation. The Generalized Logistic (GL) was the probabilities distribution function that best matched the records of weather stations in most regions (HRs 2, 3, 4, and 5), whereas the Gaucho distribution function was appropriate for HR1. Based on these distributions, the quantiles (annual precipitation values associated with a given occurrence probability value) were determined for return periods of 5, 10, 15, 20, 50, and 100 years.

The dry period analysis confirmed that the Rio Grande River basin shows meteorological drought events with an average duration between 1.7 and 2.5 years and an average periodicity (recurrence) of 3.9 to 4.5 years. According to the interval of the lengthiest drought periods found in each homogeneous region, it is considered that the longest meteorological

drought period in the basin was between 1993 and 2002 (with variations from one region to another) and that the 2011-2012 period showed the highest rainfall deficit on the analyzed period. This matches with other studies that claim the latter dry period as the worst occurring at the national level in the last seven decades.

Lastly, maps of drought occurrence probability were generated for the cited return periods, according to the expected precipitation deficit concerning the annual average, therefore, they reveal a directly proportional relationship between drought degree and period duration. The states of Chihuahua and Coahuila are the most affected regions in the basin for different return periods, where precipitation deficit levels vary in time showing deficit levels higher than 80 %. This would suggest that for 100 years return period, more than half of the basin could undergo an extraordinary drought, meaning serious implications on water resources available for different economic sectors and population.

The estimated return periods from this study are useful as a planning tool for water resources design and management, especially to create different availability and water usage scenarios within an extremely problematic region concerning its water supply-to-demand ratio. However, the solution for the problems in the basin must forcibly include the generation of binational public policies to achieve a territorial organization and a planned population growth, as well as to accomplish an efficient, rational, and sustainable use of this insufficient water resource. These actions are extremely important for future water management, as well as for fulfilling the 1944 Treaty between Mexico and the United States. Otherwise, conflicts between water users in the upper

and lower parts of the basin and on both sides of the border are expected to be overstated because of the limited availability of this valuable resource.

Greetings

This article is part of the work carried out for the PN-2017/4924 research project, sponsored by the National Council for Science and Technology (CONACYT), through the Scientific Development Projects Program in attendance to National Issues. The authors greatly appreciate the opinions and advice of three anonymous reviewers, which enhanced this research.

References

Abolverdi, J., & Khalili, D. (2010). Probabilistic analysis of extreme regional meteorological droughts by L-moments in a semi-arid environment. *Theoretical and Applied Climatology*, 102, 351-366.

Acuña, J., Felipe, O., & Fernández, C. (2015). Análisis regional de frecuencia de precipitación anual para la determinación de mapas de sequías en las cuencas Chillón, Rímac, Lurín y Alto Mantaro. *Revista Peruana Geo-Atmosférica RPGA*, 4, 93-108.

Acuña, J., Felipe, O., Ordoñez, J., & Arboleda, F. (2011). Análisis regional de frecuencia de precipitación anual para la determinación de mapas de sequías. *Revista Peruana Geo-Atmosférica RPGA*, 3, 104-115.

Alexandersson, H. (1986). A homogeneity test applied to precipitation data. *Journal of Climatology*, 6, 661-675.

Arreguín, F. I., López, M., Korenfeld, D., & Ortega-Gaucin, D. (2016a). The National Drought Policy in Mexico. *Journal of Energy Challenges and Mechanics*, 3(3), 157-166.

Arreguín, F. I., López, M., Ortega-Gaucin, D., & Ibáñez, O. (2016b). La política pública contra la sequía en México: avances, necesidades y perspectivas. *Tecnología y ciencias del agua*, 7(5), 63-76.

Arreguín, F. I., López, M., Velázquez, C., & López, R. (2013). Análisis de sequías en el marco del Tratado sobre Aguas Internacionales de 1944. *Tecnología y ciencias del agua*, 4(1), 117-148.

Báez, R., Prieto, D. V., & Aroche, R. (2016). Estudio de aplicación del análisis regional de frecuencias basado en L-momentos al caso de las precipitaciones anuales en la provincia de Camagüey, Cuba. *Revista Brasileira de Meteorología*, 31(4), 539-545.

Bass, S., Ramasamy, S., Dey-Deprick, J., & Batista, F. (2008). *Disaster risk management systems analysis*. Rome, Italy: Food and Agriculture Organization.

Brito-Castillo, L., Vivoni, E. R., Gochis, D. J., Filonov, A., Tereshchenko, L., & Monzon, C. (2010). An anomaly in the occurrence of the month of maximum precipitation distribution in northwest Mexico. *Journal of Arid Environments*, 74, 531-539.

Campos-Aranda, D. F. (2014). Análisis regional de frecuencia de crecientes en la región hidrológica no. 10 (Sinaloa), México. 2.

Contraste de predicciones locales y regionales. *Agrociencia*, 48(3), 255-270.

Carrao, H., Naumann, G., & Barbosa, P. (2016). Mapping global pattems of drought risk: An empirical framework based on sub-national estimates of hazard, exposure and vulnerability. *Global Environmental Change*, 39, 108-124.

Castillo, C., & Ortiz, N. (2015). *Regionalización de caudales máximos en la cuenca del río Sinú por medio del método estadístico índice de creciente* (Proyecto de Pregrado). Bogotá, Colombia: Universidad Santo Tomás, Facultad de Ingeniería Ambiental.

Cenapred, Centro Nacional de Prevención de Desastres. (2012). Características e impacto socioeconómico de los principales desastres ocurridos en la república mexicana en el año 2011. México, DF, México: Secretaría de Gobernación.

Cerano, J., Villanueva, J., Valdez, R. D., Méndez, J., & Constante, V. (2011). Sequías reconstruidas en los últimos 600 años para el noreste de México. *Revista Mexicana de Ciencias Agrícolas*, Pub. Esp. No. 2, 235-249.

Conagua, Comisión Nacional del Agua. (2018). *Estadísticas del agua en México.* Ciudad de México, México: Secretaría del Medio Ambiente y Recursos Naturales.

Conagua, Comisión Nacional del Agua. (2016). *Atlas del agua en México*. Ciudad de México, México: Secretaría del Medio Ambiente y Recursos Naturales.

Conagua, Comisión Nacional del Agua. (2014). *Programa de Medidas Preventivas y de Mitigación de la Sequía del Consejo de Cuenca Río Bravo*. México, DF, México: Secretaría del Medio Ambiente y Recursos Naturales.

Conagua, Comisión Nacional del Agua. (2010). *Estadísticas del agua en México*. México, DF, México: Secretaría del Medio Ambiente y Recursos Naturales.

De-la-Cruz, J., & Ortega-Gaucin, D. (18-20 septiembre, 2019). Análisis regional de frecuencia de sequía meteorológica en la zona árida de México. Artículo COMEII-19011. En: *Memorias del Quinto Congreso Nacional de Riego y Drenaje COMEII-AURPAES 2019*. Mazatlán, Sinaloa, México.

Eslamian, S., Hassanzadeh, H., Abedi-Koupai, J., & Gheysari, M. (2012). Application of L-moments for regional frequency analysis of monthly drought indexes. *Journal of Hydrologic Engineering*, 17(1), 32-42.

Esparza, M. (2014). La sequía y la escasez de agua en México. Situación actual y perspectivas futuras. *Secuencia*, 89, 195-219.

Florescano, E. (2000). *Breve historia de la sequía en México*, 2ª ed. México, DF, México: Consejo Nacional para la Cultura y las Artes.

Greenwood, J. A., Landwehr, J. M., Matalas, N. C., & Wallis, J. R. (1979). Probability weighted moments: Definition and relation to parameters of several distributions expressable in inverse form. *Water Resources Research*, 15, 1049-1054.

Guijarro, J. A. (2018). *Homogeneización de series climáticas con Climatol (Versión 3.1.1)*. Islas Baleares, España: Agencia Estatal de Meteorología.

Hallack, M. & Ramírez, J. (2010). Estudio de caso de la región noroeste de México: Sonora y Baja California. En: UNESCO (ed.). *Guía metodológica para la aplicación del análisis regional de frecuencia de sequías basado en L-momentos y resultados de aplicación en América Latina* (77 pp.) (Documentos Técnicos del PHI-LAC, No 27). Montevideo, Uruguay: Centro del Agua para Zonas Áridas y Semiáridas de América Latina y el Caribe.

Hosking, J. R. M., & Wallis, J. R. (1997). *Regional frequency analysis: An approach based on L-moments*. Cambridge, UK: Cambridge University Press.

Kalma, J. and Franks, S. (2003). Rainfall in arid and semiarid regions. In: Simmers, I. (ed.). *Understanding water in a dry environment* (pp. 15-63). Lisse, Netherlands: Balkema.

Kim, T. W., Valdés, J. B., & Aparicio, J. (2002). Frequency and spatial characteristics of droughts in the Conchos River Basin, Mexico. *Water International*, 27(3), 420-430.

La-Cruz, F. J. (2015). *Análisis de las sequías meteorológicas en Venezuela utilizando el método L-momentos* (tesis de Doctorado en Ingeniería). Bárbula, Venezuela: Universidad de Carabobo.

Linares, M. (2004). La sequía en la cuenca del río Bravo: principios de política. *Gaceta Ecológica*, 70, 57-66.

Magaña, V. O., Vázquez, J. L., Pérez, J. L., & Pérez, J. B. (2003). Impact of El Niño on precipitation in Mexico. *Geofísica Internacional*, 42(3), 313-330.

Martínez, P. F. (ed.) (2018). *La cuenca del río Bravo y el cambio climático*. San Andrés Cholula, México: Universidad de las Américas Puebla.

Montero, M., Santana, J. C., Mateos, E., & Ibáñez, O. F. (2017). Análisis de precipitación extrema para la cuenca del río Conchos, usando el Índice Normalizado de Precipitación. En: Montero, M., & Ibáñez, O. F. (coords.). *La cuenca del río Conchos: una mirada desde las ciencias ante el cambio climático* (pp. 85-107). Jiutepec, México: Instituto Mexicano de Tecnología del Agua.

Naranjo, R. C. A. (2011). *Análisis regional de frecuencia mediante el método de los L-momentos en las regiones de Valparaíso y Metropolitana para la generación de cartografía probabilística de sequía meteorológica* (Memoria de Título de Ingeniería en Recursos Naturales Renovables). Santiago de Chile, Chile: Universidad de Chile.

Norbiato, D., Borga, M., Sangati, M., & Zanon, F. (2007). Regional frequency analysis of extreme precipitation in the eastern Italian Alps and the August 29, 2003, flash flood. *Journal of Hydrology*, 345, 149-166.

Núñez-Galeano, L., & Giraldo-Osorio, J. D. (2016). Adaptation of the L-moments method for the regionalization for maximum annual temperatures in Colombia. *Ingeniería y Universidad*, 20(2), 373-389.

Núñez-López, D., Treviño-Garza, E. J., Reyes-Gómez, V. M., Muñoz-Robles, C. A., Aguirre-Calderón, O. A., & Jiménez-Pérez, J. (2013). Interpolación espacial de la precipitación media mensual en la cuenca del río Bravo/Grande. *Tecnología y ciencias del agua*, 4(2), 185-193.

Núñez-López, D., Muñoz-Robles, C. A., Reyes-Gómez, V. M., Velasco, I., & Gadsden-Esparza, H. (2007). Caracterización de la sequía a diversas escalas de tiempo en Chihuahua, México. *Agrociencia*, 41(3), 253-262.

Oliver, M. A., & Webster, R. (1990). Kriging: A method of interpolation for geographic information systems. *International Journal of Geographical Information Systems*, 4(3), 313-332.

OMM, Organización Meteorológica Mundial. (2006). *Vigilancia y alerta temprana de la sequía: conceptos, progresos y desafíos futuros.* OMM-N° 1006. Ginebra, Suiza: Organización Meteorológica Mundial.

OMM-GWP, Organización Meteorológica Mundial y Asociación Mundial para el Agua. (2016). *Manual de indicadores e índices de sequía*. Ginebra, Suiza: Organización Meteorológica Mundial y Asociación Mundial para el Agua.

Ortega-Gaucin, D. (2013). Caracterización de las sequías hidrológicas en la cuenca del río Bravo, México. *Terra Latinoamericana*, 31(3), 167-180.

Ortega-Gaucin, D., & Velasco, I. (2013). Aspectos socioeconómicos y ambientales de las sequías en México. *Aqua-LAC*, 5(2), 90-90.

Ortega-Gaucin, D., De-la-Cruz, J., & Castellano, H. V. (2018). Peligro, vulnerabilidad y riesgo por sequía en el contexto del cambio climático

en México. En: Lobato, R., & Pérez, A. (coords.). *Agua y cambio climático* (pp. 78-103). Jiutepec, México: Instituto Mexicano de Tecnología del Agua.

Paredes, F., La-Cruz, F., & Guevara, E. (2014). Análisis regional de frecuencia de las sequías meteorológicas en la principal región cerealera de Venezuela. *Bioagro*, 26(1), 21-28.

Paulhus, J. H. L., & Kohler, M. A. (1952). Interpolation of missing precipitation records. *Monthly Weather Review*, 80(8), 129-133.

Peel, M. C., Wang, Q., Vogel, R., & McMahon, T. (2001). The utility of L-moment ratio diagrams for selecting a regional probability distribution. *Hidrologycal Sciences Journal*, 46(1), 147-155.

Rodríguez, B., & Pineda-Martínez, L. F. (2017). Análisis de la variabilidad de las precipitaciones en la región transfronteriza del centro-norte de México y el sur de los Estados Unidos. En: Montero, M., & Ibáñez, O. F. (coords.). *La cuenca del río Conchos: una mirada desde las ciencias ante el cambio climático* (pp. 59-82). Jiutepec, México: Instituto Mexicano de Tecnología del Agua.

Schaefer, M. G., Barker, B. L., Taylor, G. H., & Wallis, J. R. (2007). *Regional precipitation-frequency analysis and spatial mapping for 24-hour precipitation for Oregon. Final Report SPR656*. Washington, DC, USA: MGS Engineering Consultants.

Seager, R., Ting, M., Davis, M., Cane, M., Naik, N., Nakamura, J., Li, C., Cook, E., & Stahle, D. W. (2009). Mexican drought: An observational modeling and tree ring study of variability and climate change. *Atmósfera*, 22(1), 1-31.

Semarnat, Secretaría de Medio Ambiente y Recursos Naturales. (2 de junio, 2011). Acuerdo por el que se da a conocer el resultado de los estudios técnicos de la Región Hidrológica número 24 Bravo-Conchos. *Diario Oficial de la Federación*. México, DF, México: Secretaría de Medio Ambiente y Recursos Naturales.

Stedinger, J. R., Vogel, R. M., & Foufoula-Georgiou, E. (1993). Frequency analysis of extreme events. In: Maidment, D.R. (ed.). *Handbook of hydrology* (pp: 18.1-18.66). New York, USA: McGraw-Hill.

UNESCO, Organización de las Naciones Unidas para la Educación, la Ciencia y la Cultura. (2010). *Guía metodológica para la aplicación del análisis regional de frecuencia de sequías basado en L-momentos y resultados de aplicación en América Latina*. Documentos Técnicos del PHI-LAC, No 27. Montevideo, Uruguay: Centro del Agua para Zonas Áridas y Semiáridas de América Latina y el Caribe.

Valiente, O. M. (2001). Sequía: definiciones, tipologías y métodos de cuantificación. *Investigaciones Geográficas*, 26, 59-80.

Velasco, I., Aparicio, J., Valdéz, J. B., Velázquez, J., & Kim, T. W. (2004). Evaluación de índices de sequía en las cuencas de afluentes del río Bravo/Grande. *Ingeniería Hidráulica en México*, 19(3), 37-53.

Vich, A. I., Norte, F. A., & Lauro, C. (2014). Análisis regional de frecuencias de caudales de ríos pertenecientes a cuencas con nacientes en la cordillera de los andes. *Meteorológica*, 39(1), 3-26.

Wallis, J. R., Schaefer, M. G., Barker, B. L., & Taylor, G. H. (2007). Regional precipitation-frequency analysis and spatial mapping for 24-

hour and 2-hour durations for Washington State. *Hydrology and Earth System Sciences*, 11(1), 415-442.

Wilhite, D. A. (2000). Drought as a natural hazard: Concepts and definitions. In: Wilhite, D. A. (ed.). *Drought: A global assessment*. Vol. I (pp. 3-18). New York, USA: Routledge.

Wilhite, D. A., & Glantz, M. H. (1985). Understanding the drought phenomenon: The role of definitions. *Water International*, 10, 111–120.